International Journal of Multiphase Flow 35 (2009) 963–969

Contents lists available at ScienceDirect

International Journal of Multiphase Flow

journal homepage: www.elsevier.com/locate/ijmulflow

Interaction between two spheres placed in tandem arrangement in steady and pulsating flow

L. Prahl [a], A. Jadoon [b], J. Revstedt [b,*]

[a] Department of Mechanics, Royal Institute of Technology, SE-100 44 Stockholm, Sweden
[b] Fluid Mechanics/Energy Sciences, LTH, Lund University, SE-221 00 Lund, Sweden

ARTICLE INFO

Article history:
Received 12 August 2008
Received in revised form 1 May 2009
Accepted 3 May 2009
Available online 12 May 2009

Keywords:
Dual particles
Tandem formation
Interaction
Volume of solid (VOS)

ABSTRACT

The interaction among two spheres in tandem formation are studied for a Reynolds number of 300 using both steady and pulsating inflow conditions. The purpose is to further investigate the force characteristics as well as the shedding patterns of the two spheres as the separation distance is changed from 1.5 to 12 sphere diameters. The method used for the simulations is the volume of solid (VOS) method, an approach based on the volume of fluid (VOF) method. Comparisons with other computational methods have shown VOS to accurately resolve the flow field around solid spheres. The results show that the separation distance plays a significant role in changing the flow patterns and shedding frequencies at moderate separation distances, whereas effect on drag is observed even at a separation distance of 12 diameters.

1. Introduction

The interaction of particles at moderate Reynolds numbers has various applications ranging from industrial fluidised beds, to bioreactors, to the combustion of aerosols. The understanding of the behaviour and underlying theoretical concepts of these systems is critical. Numerous studies have been carried out for flow around a single spherical particle and the different transition modes the flow undergoes with increasing Re, for example (Fornberg, 1988; Johnson and Patel, 1999; Kim and Pearlstein, 1990; Lee, 2000). At low Reynolds numbers in a uniform flow, the flow past a single sphere is attached and steady. Taneda (1956) observed the forming of steady axisymmetric vortex ring as the boundary layer separated from the particle at a Reynolds number of approximately 24. More recent studies report this first transition to occur at Re = 20 (Johnson and Patel, 1999). With an increase in Reynolds number, the recirculation downstream of the sphere is extended and becomes non-axisymmetric as the Reynolds number reaches a value of 210–212 (Johnson and Patel, 1999; Natarajan and Acrivos, 1993; Taneda, 1956; Tomboulides and Orszag, 2000). However, the flow remains steady until a third transition mode occurs, at which vortex ring stability is lost. The third transition has been reported by Natarajan and Acrivos (1993) to occur at Re = 277.5, where as Tomboulides and Orszag (2000) observed the appearance of the third mode the interval $270 \leqslant Re \leqslant 285$ and Johnson and Patel (1999) in the range $270 \leqslant Re \leqslant 280$. The flow is now unsteady however periodic. Averaged in time the flow exhibits planar symmetry around the plane where the shedding process is initiated. With the flow being periodic, a single dominating frequency corresponding to a Strouhal number (St) of 0.136 has been observed at a Reynolds number of 300 by Johnson and Patel (1999) and Tomboulides and Orszag (2000). As the Reynolds number is increased, Tomboulides and Orszag (2000) found that the flow lost its planar symmetry and became chaotic for $300 \leqslant Re \leqslant 500$. Sakamoto and Haniu (1990, 1995) reported this transition to occur for Re > 420. However, Gushchin and Matyushin (2006) observed the loss of planar symmetry at Re = 375. Mittal et al. (2001) reported that the loss of strict planar symmetry in the sphere wake at about Re = 360 is not immediately followed by the appearance of statistically axisymmetric wake. Instead the wake undergoes a transition to the mode where vortex loops are formed with preferred orientations (Re = 500, 650). However, with the increase in Re this preferred orientation diminishes and wake approaches a statistically axisymmetric state (Re = 1000).

Relatively fewer studies have been carried out considering the interaction among spheres especially in the unsteady periodic ($285 \leqslant Re \leqslant 380$) and the chaotic regimes (Re > 380). The effect of the presence of a secondary sphere placed at different separation distances and angles with respect to reference sphere on drag and lift forces, shedding frequencies and wake structures is still poorly understood. The first experimental studies regarding spheres interacting at low Reynolds number which were performed by Eveson et al. (1959), Happel and Pfeffer (1960) and Rowe and Henwood (1961). Happel and Pfeffer (1960) reported the increase in the terminal velocity for two particles falling in tandem formation

* Corresponding author. Tel.: +46 46 222 4302; fax: +46 46 222 4717.
E-mail address: johan.revstedt@energy.lth.se (J. Revstedt).

0301-9322/$ - see front matter © 2009 Elsevier Ltd. All rights reserved.
doi:10.1016/j.ijmultiphaseflow.2009.05.001

compared to an isolated particle. More recent works have extended this to relatively large Reynolds number in order to examine the dependency of wake structure, flow separation, shedding frequencies and drag effects on inter-sphere distance and Reynolds number. However, the majority of these studies are focused on spheres in side-by-side arrangement, e.g. Kim et al. (1993), Brydon and Thompson (2001), Folkersma et al. (2000) and Schouveiler et al. (2004). However, both tandem and side-by-side formation have been investigated experimentally by Chen and Lu (1999) and numerically by Tsuji et al. (2003). Liang et al. (1996) reported the results for drag using four different spheres arrangements. Zou et al. (2005) investigated the flow patterns and shedding frequencies at different separation distances when studying wake structure interaction for dual spheres placed in tandem. In a recent study Yoon and Yang (2007) investigated the interaction of a pair of spheres a Re = 300 varying both the separation distance and the angular position relative to the flow direction.

All the above mentioned studies point out the importance of the separation distance and position of the secondary sphere which in turn significantly affect drag, lift and the shedding patterns. For spheres in tandem formation, as the gap between the sphere is decreased, the reference (upstream) particle undergoes an increase in drag caused by the interaction of the high-pressure region in front of the secondary (downstream) sphere with the low-pressure region behind the reference sphere resulting in a 'slipstream effect', i.e. the secondary sphere experiences a smaller flow velocity that leads to a larger drag force for leading particle. However, the drag of the reference sphere is still smaller compared to the drag of a single sphere. As the separation distance is increased, the drag force gradually levels off to the value of an isolated sphere. The parameter which is most significantly affecting the drag force for tandem arrangement appears to be if the secondary sphere is positioned in the recirculation part of the wake of the reference sphere or not Olsson and Fuchs, 1998; Zhu et al., 1994. Spheres positioned in tandem are not subjected to any lift force for Reynolds number less than 200, e.g. Prahl et al. (2007). For moderate Reynolds number (300), the wake behaves as steady and axisymmetric, steady and plane symmetric and finally unsteady as separation distance between two spheres is increased from 1.5 to 2.5D. At a gap of 3–4D, the wake undergoes a three-dimensional transition. Further increasing the separation distance the wake will re-assume planar symmetry (Zou et al., 2005).

The motivation for the present work is based on obtaining better understanding of the phenomena occurring in the interaction of spheres in the unsteady wake region. A major purpose of the present study is to use the results in order to improve the Eulerian–Lagrangian models for particle laden flows, so as to account for the effects of non-colliding particle interactions on the force loading. Hence, the results obtained here will be used to adjust the drag and lift models currently used in Eulerian–Lagrangian models. In a previous study (Prahl et al., 2007), we investigated particle interactions in the stationary wake flow regime. The present work is an extension towards higher Reynolds numbers and thereby entering the unsteady wake regime. Both steady and time dependent inflow conditions are used. The reason for including a time dependent inflow is to be able to investigate how the wake and the forces respond to flow unsteadiness.

2. Numerical method

The continuity and momentum equations governing an isothermal, incompressible flow of a Newtonian fluid are spatially discretised using first and second order basic finite-difference schemes on a staggered Cartesian grid. A single step defect correction method (Gullbrand et al., 2001) is used to improve the accuracy without loosing any numerical stability to third order for convective terms and fourth order for remaining terms. A second order fully implicit scheme is used for temporally discretisation of the transient terms. The resulting system of algebraic equations is solved using a multigrid method where the pressure–velocity coupling is done through simultaneous update of dependent variables as the continuity equation is relaxed (Fuchs and Zhao, 1984).

2.1. Volume of solid (VOS)

The volume of solid (VOS) method (Lörstad and Fuchs, 2001) is used to describe complex surfaces on a Cartesian grid. It is derived from the volume of fluid (VOF) approach in which the amount of fluid and solid in each cell is defined. For reasons of simplicity we now consider a two-dimensional flow over a flat fluid–fluid interface. The velocity derivatives will in general have different values on either side of the interface. However, the shear stress will be equal on either side of the interface. In this two-dimensional example the shear stress at the interface is then determined by

$$\tau_{xy} = \mu^{(k)}\left(\frac{\partial u^{(k)}}{\partial y} + \frac{\partial v^{(k)}}{\partial x}\right) \tag{1}$$

where $k = 1, 2$ denotes the fluid. In the VOF approach one often assumes a linear relationship between amount of each fluid in a cell and the average viscosity of that cell (Rudman, 1998; Puckett et al., 1997). Hence, the viscosity in a cell can be calculated from:

$$\mu = \alpha\mu^{(1)} + (1-\alpha)\mu^{(2)} \tag{2}$$

where α is the phase variable representing the amount of fluid in each cell, $(0 \leqslant \alpha \leqslant 1)$. Using the VOF method we may write the shear stress as

$$\tau_{xy} = \mu\left(\alpha\left[\frac{\partial u^{(1)}}{\partial y} + \frac{\partial v^{(1)}}{\partial x}\right] + (1-\alpha)\left[\frac{\partial u^{(2)}}{\partial y} + \frac{\partial v^{(2)}}{\partial x}\right]\right) \tag{3}$$

Combining Eqs. (1) and (2) the following expression for the dynamic viscosity in a cell is obtained:

$$\mu = \frac{1}{\frac{\alpha}{\mu^{(1)}} + \frac{1-\alpha}{\mu^{(2)}}} \tag{4}$$

which is the harmonic mean of the dynamic viscosity. Letting the viscosity of the second fluid (i.e the solid) in Eq. (4) go to infinity and assuming constant density a simple expression for the kinematic viscosity ratio $(\delta\nu)$ in a cells cut by the interface can be formed.

$$\delta\nu = \frac{\nu}{\nu^{(1)}} = \frac{\mu}{\mu^{(2)}} = \frac{1}{\alpha} \tag{5}$$

Cells containing only solid phase will be blocked as there will be no flow $(\alpha = 0)$ in these cells. Thus no computation will be carried out for these cells. Further details regarding the technique used to represent the constant shear stress can be found in Lörstad and Fuchs (2001).

With the definition of viscosity ratio from Eq. (5), the governing equations for an incompressible flow can, on a non-dimensional form, be written as

$$\frac{\partial u_i}{\partial x_i} = 0 \tag{6}$$

$$\frac{\partial u_i}{\partial t} + u_j\frac{\partial u_i}{\partial x_j} = -\frac{\partial p}{\partial x_i} + \frac{1}{\mathrm{Re}}\frac{\partial}{\partial x_j}\left(\delta\nu\left[\frac{\partial u_i}{\partial x_j} + \frac{\partial u_j}{\partial x_i}\right]\right) \tag{7}$$

where u_i is the velocity, p is the pressure and $\delta\nu$ the viscosity ratio.

By integrating the momentum equations over a control volume and then transforming the volume integral into a surface integral using Gaussian theorem the following equation is obtained:

$$F_i = \int\int_{\Omega}\int \frac{\partial u_i}{dt} d\Omega + \int\int_{\Gamma}\left(u_i u_j n_j + p n_i - \delta v \frac{1}{Re}\left[\frac{\partial u_i}{\partial x_j} + \frac{\partial u_j}{\partial x_i}\right] n_j\right) d\Gamma \quad (8)$$

where Γ represents the outer surface of a control volume, n_i is the unit vector normal to the surface and $\delta v = 1$ on the boundary Γ. The forces acting on the object is obtained by applying Eq. (8) on the faces of the control volume.

3. Problem set-up

Two equally sized spheres with a diameter D are held fixed in a rectangular domain while changing the relative position in tandem between the spheres. For the dual sphere formations, the leading sphere, named the "reference sphere", is fixed at $10D$ downstream of the inlet, while the position of the trailing sphere, denoted the "secondary sphere", is defined by the separation distance D_0 using $D_0 = 1.5, 2, 3, 6, 9, 12D$ and $D_0 = 1.5, 2, 3, 4.5, 6$ for the steady and pulsating inflow profiles, respectively (see Fig. 1). The Reynolds numbers is 300 in all simulations. At the inlet, a uniform velocity profile, stationary as well as pulsating is applied. The pulsating inflow is a periodic modulation of the uniform inlet velocity, where the amplitude of the fluctuations is $0.1U_{\text{in}}$, pulsating with Strouhal numbers ($\text{St}_{\text{in}} = fD/U_{\text{in}}$) of 0.1, 0.135 and 0.2. $\text{St}_{\text{in}} = 0.135$ is chosen due to the fact that it is close to the natural frequency connected to Re = 300 whereas the other two frequencies are tested in order to study the impact of a slight change in frequency with respect to the natural frequency. A grid resolution of $h = D/64$ is used for all simulations with a domain size of $[32,32,64]D$ (Fig. 1). A study of the grid dependency can be found in Electronic Annex 1 of the online version of this article. The results are presented in terms of time averaged drag and lift coefficients (C_D, C_L) and in terms of the standard deviations of the drag and lift coefficient fluctuations ($\Delta C_D, \Delta C_L$). These the instantaneous force coefficients were sampled at every time step and the statistics were calculated according to Eqs. (9) and (10) over at least 150 time units after the flow had reached statistical steady state, which corresponds to about 20 shedding periods at a shedding frequency St = 0.135.

$$C_D = \frac{1}{N}\sum_{n=1}^{N}(\widehat{C}_D)_n \quad (9)$$

$$\Delta C_D = \sqrt{\frac{1}{N}\sum_{n=1}^{N}[(\widehat{C}_D)_n - C_D]^2} \quad (10)$$

The "$\widehat{\cdot}$" denotes instantaneous values and N is the number of time steps.

4. Results

Simulations have been performed for both a single sphere and dual spheres in tandem at a Reynolds number of 300.

Fig. 2a shows the mean drag coefficient for both spheres at steady inflow. The greatest drag reduction is found at a separation distance of $D_0 = 3D$. By further increasing the separation distance, the drag levels off to that of a single sphere for separation distances larger than $6D$. The secondary sphere experiences a minimum drag at $D_0 = 1.5D$ that is slowly increasing as the separation distance is increased. However, even at a separation distance of $12D$, the drag force is still only about 80% of that of a single sphere. Also added to Fig. 2a are the results of Yoon and Yang (2007), and, as can be seen, our results agree very well with theirs. It is worth noting that the fluctuations of drag and lift for the reference sphere are significantly smaller than for the single sphere case, whereas the drag coefficient fluctuations on the secondary sphere is up to seven times larger than that of the single sphere. The former is probably caused by a phenomenon similar to the one found in previous studies for dual particle formations in lower Reynolds number flows ($\leqslant$200), (Olsson and Fuchs, 1998; Prahl et al., 2007), where the inclusion of a secondary particle placed in the proximity of a reference sphere will delay the development of the wake behind the reference sphere. Hence, the presence of the secondary sphere will both dampen and delay the vortex shedding on the reference sphere. Regarding the latter, the increase in drag fluctuations for the secondary sphere is caused by the vortex shedding on the reference sphere. At the shorter separation distances ($2.5D$ and $3D$) we observe no shedding from the secondary sphere. Instead a toroidal vortex is formed which is periodically disrupted by the vortex shed by the reference sphere. At $D_0 = 2.5D$ this disruption occurs twice per shedding cycle, first due to collision with the reference sphere vortex and secondly by what appears to be a "suction" effect as the reference sphere vortex is passing. This can be clearly seen in Electronic Annex 2 of the online version of this article, showing a λ_2-visualisation of the vortex structures. Considering a similar visualisation at $D_0 = 3D$ (Electronic Annex 3) one can see the interaction of the vortices are somewhat different. Here the toroidal vortex barely has time to reform before it is hit by the reference sphere vortex. One can also observe an oscillating motion of the wake in the gap between the spheres. This leads to an alternating shedding position which in turn results in the zero mean lift noted in Fig. 2b. At $D_0 = 6D$ shedding from both spheres is observed and the interaction of these vortices creates a fairly complex wake structure downstream of the secondary sphere, as can be seen in Electronic Annex 4 of the online version of this article.

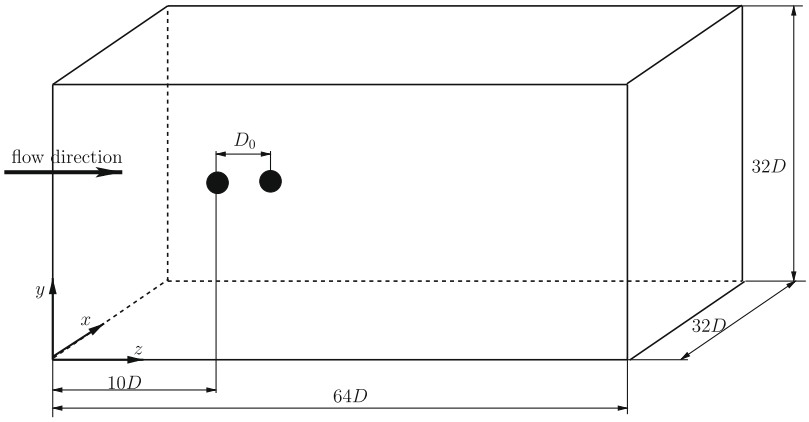

Fig. 1. The computational domain and coordinate system.

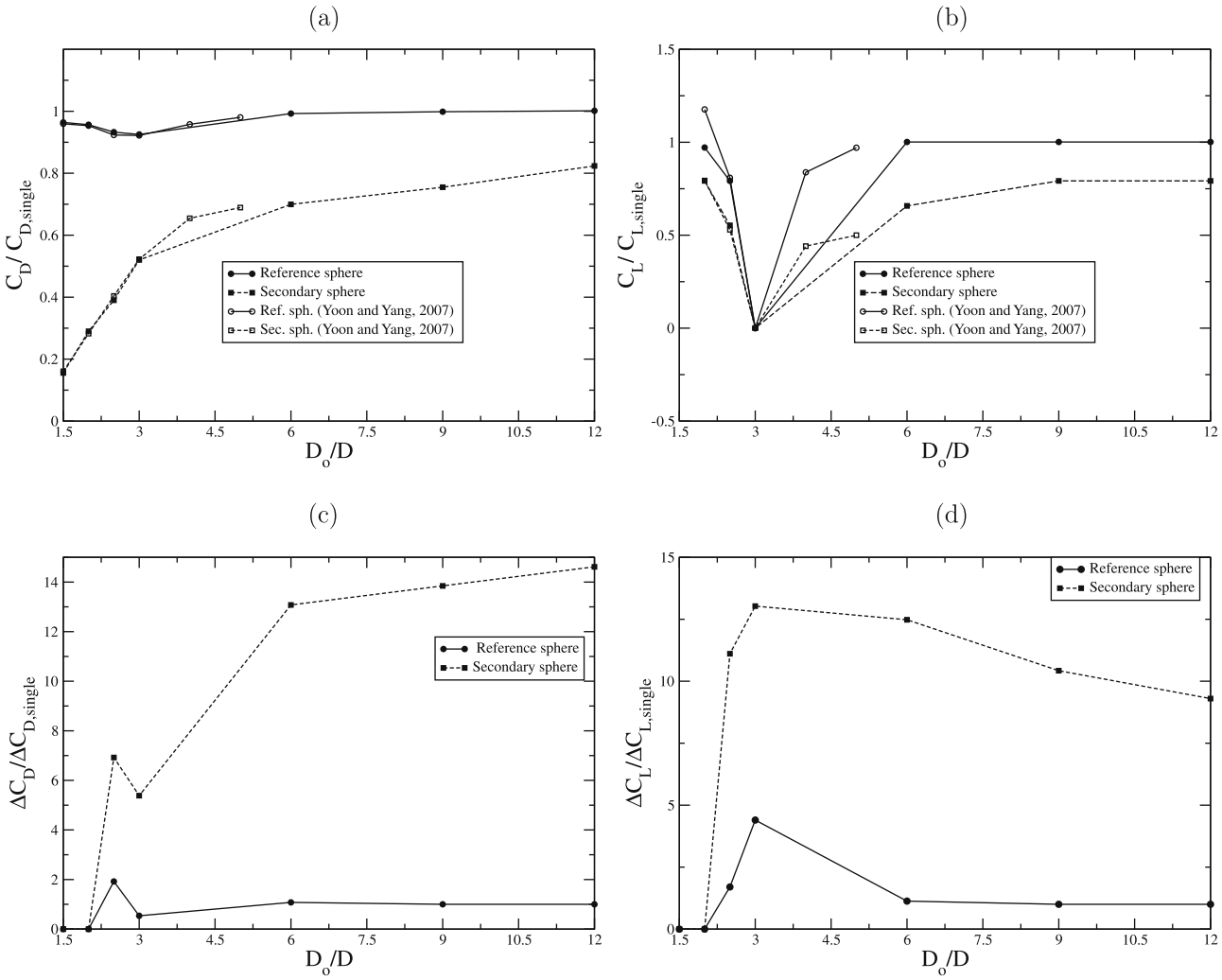

Fig. 2. The absolute value of mean C_D (a) and the absolute value of mean C_L (b) compared with the results of Yoon and Yang (2007) and the rms of the fluctuations thereof; ΔC_D (c), ΔC_L (d) as a function of the separation distance for both the reference and the secondary sphere at Re = 300, for steady inflow.

Considering the pulsating inflow conditions in Fig. 3a, the mean drag shows a behaviour similar to that of the steady inflow condition case, However, the point of maximum drag reduction is dependent on the frequency of the inflow velocity. As the frequency is increased this point is moved upstream. For the secondary sphere, all cases show similar behaviour. The smallest separation distance leads to the greatest drag reduction, a reduction that is decreasing as the separation distance is increased. The case with $St_{in} = 0.135$ is most similar to the steady inflow case, whereas $St_{in} = 0.1$ shows a similar trend as the former two but with an enhanced drag reduction. Furthermore, one may also notice the very large fluctuations in the drag, Fig. 3c, mostly originating from the fact that the inflow velocity varies periodically.

A decrease in mean lift coefficient (Fig. 2b from a value close to that of a single sphere at $D_0 = 2D$ to almost zero at $D_0 = 3D$ is observed for the reference sphere in the steady inflow case, which is also noted by Yoon and Yang (2007). Further increasing the separation distance, the mean lift coefficient again increases and approaches the single sphere value for $D_0 \geqslant 6D$. A similar trend is observed for the secondary sphere, however the values are somewhat lower except at $D_0 = 3D$. By comparing Figs. 2b and 3b it is evident that the lift of the pulsating inflows is much lower than for the steady case, especially at large separation distances. This may be caused by the difference in shedding patterns, as the periodicity of the natural shedding competes with the shedding of an axisymmetric vortex, which in turn will decrease the asymmetry in the wake and hence also the lift force. For a separation distance of $D_0 = 2D$, relatively large lift values are observed, Fig. 3b. This is probably due to the asymmetry in the shedding caused by the periodicity of the inflow. Considering Figs. 2d and 3d, the lift fluctuations of the reference sphere is to a greater extent affected by the pulsating inflow for all separation distances compared to the steady inflow case. For the secondary sphere, the lift fluctuations are, in the pulsating inflow cases, less affected by the inflow condition. At short separation distances the lift fluctuations are larger for the higher inflow frequency. However, beyond $D_0 = 4.5D$ the situation is opposite.

Increasing the separation distance in steady inflow from $1.5D$ to $2D$ the wake transforms from steady axisymmetric to steady plane symmetric. A further increase in separation distance to $2.5D$ results in a unsteady plane symmetric flow. Up to $D_0 = 2.5D$ our results resemble the findings of Zou et al. (2005). However, for a separation distance of $3D$ Zou et al. (2005) observed a symmetry plane, while our results indicate that the flow is statistically axisymmetric at this separation distance. Further increasing the separation distance to $6D$, $9D$ and $12D$ leads to unsteady plane symmetric behaviour of the flow. The frequencies for steady inflow are summarised in Table 1 For the steady inflow case, both the reference

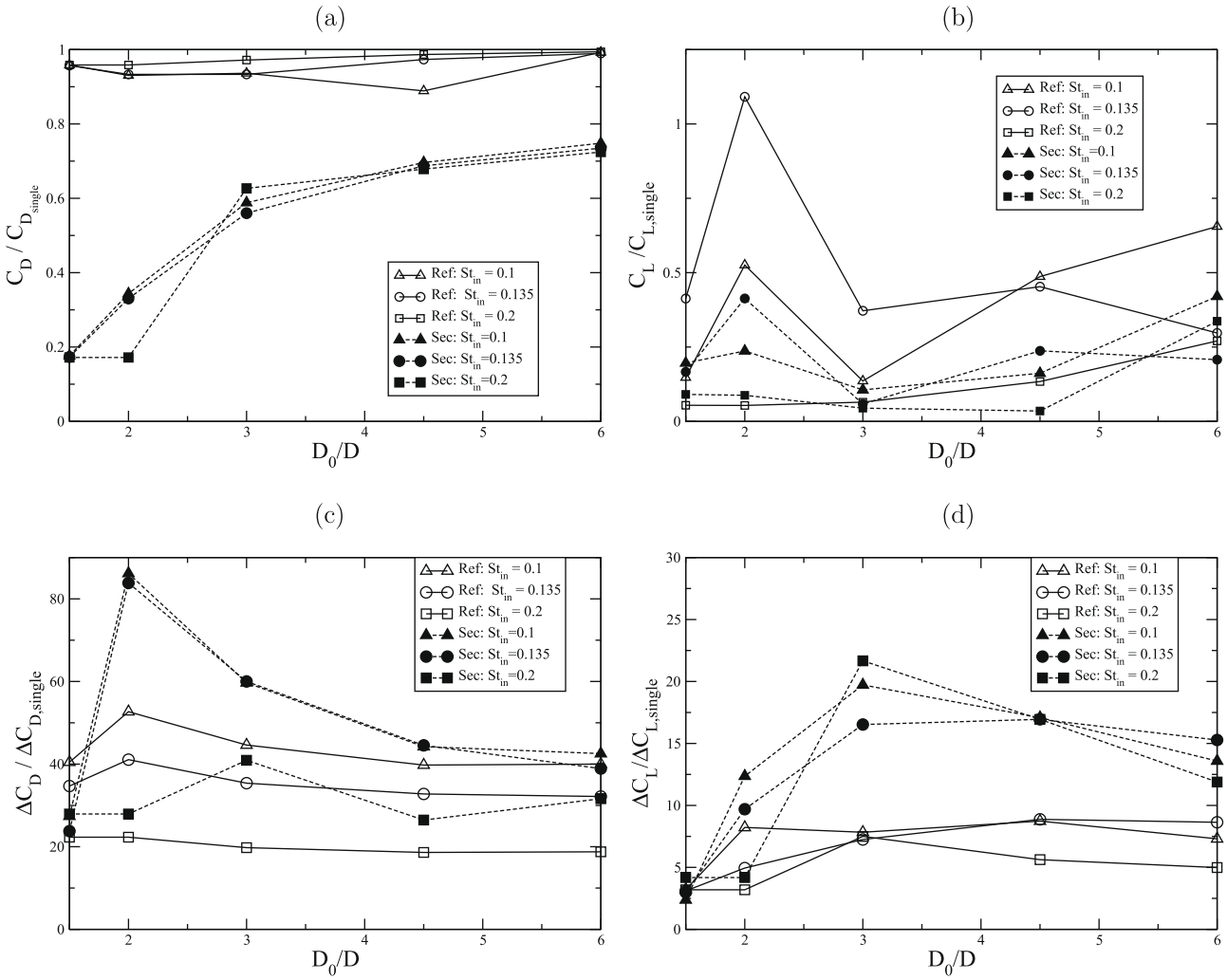

Fig. 3. Absolute value of mean C_D (a), absolute value of mean C_L (b) and the rms of the fluctuations thereof; ΔC_D (c), ΔC_L (d) as a function of the separation distance for both the reference and the secondary sphere at Re = 300, for pulsating inflow (St_{in} = 0.1, 0.135 and 0.2).

and secondary sphere have a shedding frequency a Strouhal number of approximately 0.1 at separation distances of 2.5*D* and 3*D*. For separation distances of 6*D* and above, both spheres have a Strouhal number of 0.137, i.e. equivalent to that found for a single sphere. However, with increasing separation distance, several harmonics are detected as well as enhanced for the secondary sphere, which is due to the vortex interaction discussed above and shown in Electronic Annex 4. Referring to the discussion above on the vortex interactions it can be concluded that for the unsteady wakes the terms *planar symmetric* and *axisymmetric* are insufficient to fully characterise the wakes. Therefore, to further characterise the dynamics of the wake we use the components of the instantaneous lift coefficient (C_{L_x} and C_{L_y}). Four regimes can then be identified and we refer to these as: *unidirectional* (Fig. 4a) for which the lift is varying in magnitude but the direction is always along a line; *cyclic* for which both the direction and the magnitude of the lift coefficient varies periodically; *semi-chaotic* (Fig. 4c) for which the lift has a preferred direction but with a random fluctuation around this direction, *chaotic* (Fig. 4d) for which the variation is random and no preferred direction is present. These are summarised in Table 2 for all cases. In all cases with steady inflow the wake shows a unidirectional behaviour.

For the pulsating inflow the situation is slightly different. The inflow frequency together with the separation distance determines

Table 1
Comparison of the mean drag coefficient, drag coefficient fluctuations and Strouhal numbers for spheres in tandem configuration at Re = 300, with steady inflow. The dominant frequencies are shown in bold text.

D_0	C_D(Ref)	ΔC_D	St	C_D(sec)	ΔC_D	St
1.5	0.645	–	–	0.103	–	–
2	0.64	–	–	0.194	–	–
2.5	0.621	0.0025	**0.1**, 0.2, 0.3	0.267	0.0094	**0.1**, 0.2, 0.3
3	0.619	0.0007	**0.1**	0.347	0.007	**0.1**, 0.3
6	0.669	0.0014	**0.137**, 0.26	0.473	0.017	**0.137**, 0.26, 0.39, 0.52
9	0.669	0.0013	**0.137**,0.26	0.518	0.019	**0.137**, 0.26, 0.39, 0.52, 0.65
12	0.669	0.00128	**0.137**, 0.26	0.55	0.018	**0.137**, 0.26, 0.39, 0.52, 0.65, 0.78

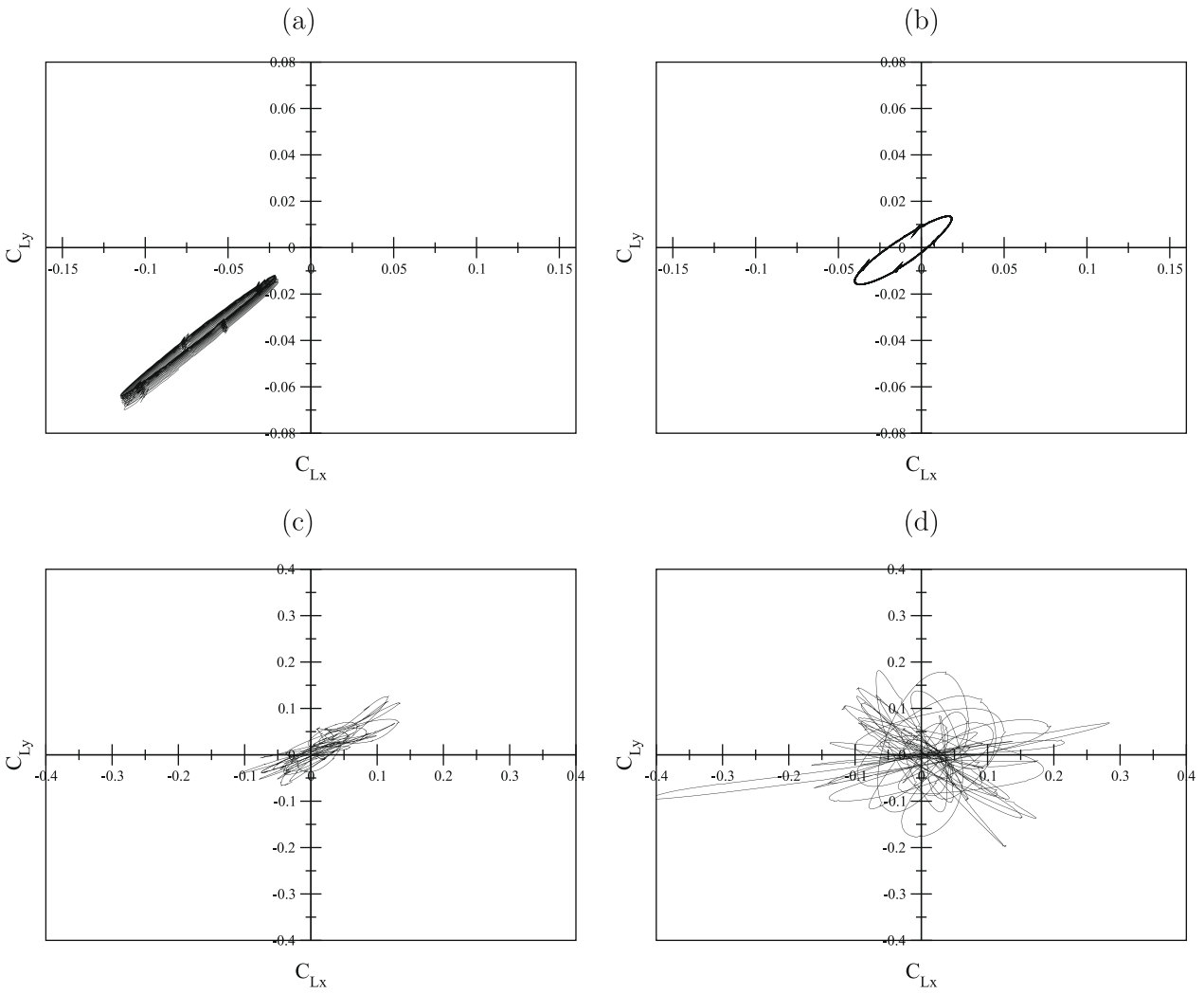

Fig. 4. Four characteristic behaviour of C_L found for spheres placed in a pulsating inflow. (a) Strict planar symmetric ($D_0 = 2D, St_{in} = 0.2$), (b) 'cyclic' planar symmetric ($D_0 = 1.5D, \mathrm{St}_{in} = 0.1$), (c) semi-chaotic ($D_0 = 4.5D, \mathrm{St}_{in} = 0.1$) and (d) chaotic ($D_0 = 2D, \mathrm{St}_{in} = 0.1$).

Table 2
The flow character depending on inflow Strouhal number and separation distance.

St	1.5*D*	2*D*	3*D*	4.5*D*	6*D*
Steady	N/A	N/A	Unidirectional	*No data*	Unidirectional
0.1	Cyclic	Chaotic	Semi-chaotic	Semi-chaotic	Semi-chaotic
0.135	Cyclic	Cyclic	Semi-chaotic	Semi-chaotic	Semi-chaotic
0.2	Cyclic	Unidirectional	Unidirectional	Unidirectional	Unidirectional

whether the flow becomes axi- or plane symmetric as well as which frequency will be dominating in the flow field. It should be noted that although all these cases are are time dependent due to the nature of the boundary conditions they are not necessarily unsteady in the sense that vortex shedding will occur, as is shown below. Particles placed 1.5*D* apart will independent of inflow frequency, have a lift behaviour corresponding to Fig. 4b. Although the wake is stable, in the sense that there is no vortex shedding present, as for the steady inflow case, there apparently some asymmetry present which generates a variation in the direction of the lift. Hence, the force fluctuations are not only caused by the temporal variation of the inflow velocity. Further increasing the separation distance leads to a situation different situations depending on inflow frequency. A general observation is that if the inflow frequency is lower or equal to the single sphere shedding frequency the wake becomes chaotic at some point where after it is, to a certain extent, stabilised and transforms to a semi-chaotic behaviour as the separation is increased. For the high frequency inflow the wake will, after being cyclic at 1.5, adopt a unidirectional behaviour similar to the steady inflow case.

Table 3 presents the Strouhal numbers of the lift force fluctuations for both spheres for the pulsating inflows. A general trend for the pulsating cases is that the frequency is locked-on to the inflow frequency. This is most evident for the smallest separation distances ($D_0 = 1.5D$). The onset of vortex shedding is at $D_0 = 2D$, where the axisymmetric vortex in the wake of the reference sphere is periodically shed. As the vortex passes around the secondary sphere, it is deformed into a hairpin vortex. Some tendency to form a hairpin vortex already in the wake of the reference sphere is also observed. This is probably the origin of the St = 0.126 observed for

Table 3
Comparison of Strouhal number for both spheres at Re = 300 placed in tandem formation for inflow frequencies (St_{in}) of 0.1, 0.135 and 0.2. Inflow frequencies are marked with bold phase in the Strouhal number column. The frequencies are organised with the strongest frequency first.

D_0	St_{in}	St_{ref}	St_{sec}
	0.1	**0.1**	**0.1**
1.5	0.135	**0.135**, 0.270	**0.135**, 0.270, 0.405
	0.2	**0.2**, 0.4	**0.2**, 0.4, 0.6
	0.1	0.030, **0.1**, 0.126	**0.1**, 0.126, 0.2
2	0.135	0.136, 0.271	0.136, 0.271, 0.169
	0.2	**0.2**	**0.2**, 0.4
	0.1	**0.1**, 0.037, 0.139	**0.1**, 0.139
3	0.135	0.136, 0.093	0.138, 0.175, 0.127, 0.093
	0.2	0.1, **0.2**, 0.3	0.1, **0.2**, 0.3
	0.1	0.035, **0.1**, 0.136	0.136, **0.1**, 0.236, 0.2
4.5	0.135	0.036, 0.136	0.170, 0.136
	0.2	0.1, **0.2**	0.1, **0.2**, 0.3, 0.5
	0.1	**0.1**, 0.041, 0.139	0.139, **0.1**, 0.24, 0.2, 0.278
6	0.135	0.034, **0.135**, 0.1	0.169, 0.3, 0.1, **0.135**
	0.2	0.1, **0.2**	0.1, 0.3, **0.2**

$St_{in} = 0.1$. Moreover, for the reference sphere in this sphere configuration, $D_0 = 2D$ and $St_{in} = 0.1$, the most dominant frequency is approximately 0.03. The same frequency is also found for the secondary sphere, although not as significant, implying that this is a resonance phenomenon. Increasing the inflow Strouhal number to 0.2, the shedding is locked-on to this frequency since the natural shedding is slower and therefore has no time to develop. Further increasing the separation distance will promote the wake development of the reference sphere leading to a behaviour which resembles that of a single sphere. The vortices shed from the reference sphere will be distorted by the secondary sphere and interact with its wake creating a fairly complex flow structure which is indicated by the frequency content for $D_0 \geqslant 3D$. It should be noted though, that we do not observe any frequencies on the secondary sphere that is not directly influenced by the upstream wake until separation distances of 4.5D and above.

5. Conclusions

The wake structures as well as the forces acting on a sphere are influenced by the presence of a second sphere. At small separation distances and steady inflow, the wake is steady. As the distance is increased vortex shedding appears first on the reference sphere. i In terms of force coefficient fluctuations the variation is weaker on the reference sphere compared to the case of a single sphere. For the secondary sphere the situation is the opposite. The fluctuations of both lift and drag are substantially larger than for a single sphere, due to the unsteadiness of the flow on this sphere. Also, the secondary sphere has only a minor influence on the mean drag force of the reference sphere. The secondary sphere though, experiences a substantial drag reduction, especially at short separation distances, but even placed 12D downstream of the reference sphere the drag is reduced by 20% compared to a single sphere. Introducing a periodic inflow further adds to the complexity of the wake structures and changes the shedding behaviour as well as the level of force fluctuations. However, the mean drag is almost unaffected by this periodicity.

Acknowledgements

The financial support for this work by the Swedish Research Council (Vetenskapsrådet) and the Centre for Combustion Science and Technology CECOST (SSF) is gratefully acknowledged. Computational resources were provided by the Swedish National Infrastructure for Computing (SNIC) and the Centre for Scientific Computing at Lund University (LUNARC).

Supplementary data

Supplementary data associated with this article can be found, in the online version, at doi:10.1016/j.ijmultiphaseflow.2009.05.001.

References

Brydon, A.D., Thompson, M.C., 2001. Flow interaction between two spheres at moderate Reynolds numbers. In: 14th Australasian Fluid Mech. Conf., December 10–14, Adelaide, Australia.
Chen, R.C., Lu, Y.N., 1999. The flow characteristics of an interactive particle at low Reynolds numbers. Int. J. Multiphase Flow 25, 1645–1655.
Eveson, G.F., Hall, E.W., Ward, S.G., 1959. Interaction between two equal-sized equal-settling spheres moving through a viscous liquid. Brit. J. Appl. Phys. 10, 43–47.
Folkersma, R., Stein, H.N., van de Vosse, F.N., 2000. Hydrodynamic interactions between two identical spheres held fixed side by side in a uniform stream directed perpendicular to the line connecting the spheres' centres. Int. J. Multiphase Flow 26, 877–887.
Fornberg, B., 1988. Steady viscous flow past a sphere at high Reynolds numbers. J. Fluid Mech. 190, 471–489.
Fuchs, L., Zhao, H.-S., 1984. Solution of three-dimensional viscous incompressible flows by a multi-grid method. Int. J. Num. Meth. Fluids 4, 539–555.
Gullbrand, J., Bai, X.-S., Fuchs, L., 2001. High-order cartesian grid method for calculation of incompressible turbulent flows. Int. J. Num. Meth. Fluids 36, 687–709.
Gushchin, V.A., Matyushin, R.V., 2006. Vortex formation mechanisms in the wake behind a sphere for $200 < Re < 380$. Fluid Dyn. 41, 795–809.
Happel, J., Pfeffer, R., 1960. The motion of two spheres following each other in a viscous fluid. AIChE J. 6, 129–133.
Johnson, T.A., Patel, V.C., 1999. Flow past a sphere up to a Reynolds number of 300. J. Fluid Mech. 378, 19–70.
Kim, I., Elghobashi, S., Sirignano, W., 1993. Three-dimensional flow over two spheres placed side by side. J. Fluid Mech. 246, 465–488.
Kim, I., Pearlstein, J., 1990. Stability of the flow past a sphere. J. Fluid Mech. 211, 73–93.
Lee, S., 2000. A numerical study of the unsteady wake behind a sphere in a uniform flow at moderate Reynolds numbers. Comput. Fluids 29, 639–667.
Liang, S.-C., Hong, T., Fan, L.-S., 1996. Effects of particle arrangements on the drag force of a particle in the intermediate flow regime. Int. J. Multiphase Flow 22, 285–306.
Lörstad, D., Fuchs, L., 2001. A volume of fluid (vof) method for handling solid objects using fixed cartesian grids. In: Moving Boundaries VI – Computational Modelling of Free and Moving Boundary Problems. Wessex Inst. of Techn., pp. 143–152.
Mittal, J., Wilson, J., Najjar, F., 2001. Symmetry properties of the transitional sphere wake. AIAA J. 40, 579–582.
Natarajan, R., Acrivos, A., 1993. The instability of the steady flow past spheres and disks. J. Fluid Mech. 254, 323–344.
Olsson, P.J., Fuchs, L., 1998. The interaction of spherical particles in a fluid flow governed by Navier–Stokes equations. In: ECCOMAS. John Wiley & Sons Ltd., pp. 180–185.
Prahl, L., Hölzer, A., Arlov, D., Revstedt, J., Sommerfeld, M., Fuchs, L., 2007. On the interaction between two fixed spherical particles. Int. J. Multiphase Flow 33, 707–725.
Puckett, E.G., Almgren, A.S., Bell, J.B., Marcus, D.L., Rider, W.J., 1997. A high-order projection method for tracking fluid interfaces in variable density incompressible flows. J. Comput. Phys. 130, 269–282.
Rowe, P.N., Henwood, G.A., 1961. Drag forces in a hydraulic model of a fluidised bed – part 1. Trans. Instn. Chem. Eng. 39, 43–54.
Rudman, M., 1998. A volume-tracking method for incompressible multifluid flows with large density variations. Int. J. Num. Meth. Fluids 28, 357–378.
Sakamoto, H., Haniu, H., 1990. A study on vortex shedding from spheres in a uniform flow. Trans. ASME J. Fluids Eng. 112, 386–392.
Sakamoto, H., Haniu, H., 1995. The formation mechanism and shedding frequency of vortices from a sphere in a uniform shear flow. J. Fluid Mech. 287, 151–171.
Schouveiler, L., Brydon, A., Leweke, T., Thompson, M.C., 2004. Interactions of the wakes of two spheres placed side by side. Eur. J. Mech. B/Fluids 23, 137–145.
Taneda, S., 1956. Experimental investigation of the wake behind a sphere at low Reynolds number. J. Phys. Soc. Jpn. 11, 1104–1108.
Tomboulides, A.G., Orszag, S.A., 2000. Numerical investigation of transitional and weak turbulent flow past a sphere. J. Fluid Mech. 416, 45–73.
Tsuji, T., Narutomi, R., Yokomine, T., Ebara, S., Shimizu, A., 2003. Unsteady three-dimensional simulation of interactions between flow and two particles. Int. J. Multiphase Flow 29, 1431–1450.
Zhu, C., Liang, S.-C., Fan, L.-S., 1994. Particle wake effects on the drag force of an interactive particle. Int. J. Multiphase Flow 20, 117–129.
Zou, J.-F., Ren, A.-L., Deng, J., 2005. Study on flow past two spheres in tandem arrangement using a local mesh refinement virtual boundary method. Int. J. Num. Meth. Fluids 49, 465–488.
Yoon, D.-H., Yang, K.-S., 2007. Flow-induced forces on two nearby spheres. Phys. Fluids 19, 098103-1–098103-4.